

Room-temperature exciton-polariton condensation in pressed perovskite microcavities

Tianyin Zhu(朱天寅), Zelei Chen(陈泽磊), Xiaoyu Wang(王小宇), Zhongmin Huang(黄钟民), Haibin Zhao(赵海斌), and Jun Wang(王俊)

Citatio: Chin. Phys. B, 2025, 34 (**9**): 094202. DOI: 10.1088/1674-1056/addce6
http://cpb.iphy.ac.cn; http://iopscience.iop.org/cpb

What follows is a list of articles you may be interested in

Quantitative determination of modal photon number density spectrum in arbitrary dielectric structures with a quantum emitter

Li-Heng Chen(陈立恒), Fengfeng Luo(罗凤凤), and Yonggui Gao(高勇贵)
Chin. Phys. B, 2025, 34 (**4**): 044204. DOI: 10.1088/1674-1056/adb262

Coherent feedback ground-state cooling of mechanical resonators assisted by a quantum well

Qinghong Liao(廖庆洪), Songyun Ouyang(欧阳嵩沄), Shaoping Cheng(程绍平), and Yiping Cheng(程依萍)
Chin. Phys. B, 2025, 34 (**4**): 044202. DOI: 10.1088/1674-1056/adb266

A novel dual-channel thermo-optic locking method for the whispering gallery mode microresonator

Wenjie Fan(范文杰), Wenyao Liu(刘文耀), Ziwen Pan(潘梓文), Rong Wang(王蓉), Lai Liu(刘来), Enbo Xing(邢恩博), Yanru Zhou(周彦汝), Jun Tang(唐军), and Jun Liu(刘俊)
Chin. Phys. B, 2024, 33 (**5**): 054206. DOI: 10.1088/1674-1056/ad225f

Efficient transfer of metallophosphor excitons via confined polaritons in organic nanocrystals

Wenbin Lu(芦文斌), Yongcong Chen(陈永聪), Xuyun Yang(杨旭云), and Ping Ao(敖平)
Chin. Phys. B, 2023, 32 (**10**): 104212. DOI: 10.1088/1674-1056/acf03b

Resonantly driven exciton Rabi oscillation in single quantum dots emitting at 1300 nm

Yong-Zhou Xue(薛永洲), Ze-Sheng Chen(陈泽升), Hai-Qiao Ni(倪海桥), Zhi-Chuan Niu(牛智川), De-Sheng Jiang(江德生), Xiu-Ming Dou(窦秀明), Bao-Quan Sun(孙宝权)
Chin. Phys. B, 2017, 26 (**8**): 084202. DOI: 10.1088/1674-1056/26/8/084202

SPECIAL TOPIC — Exciton physics: Fundamentals, materials and devices

Room-temperature exciton-polariton condensation in pressed perovskite microcavities

Tianyin Zhu(朱天寅)[1], Zelei Chen(陈泽磊)[1], Xiaoyu Wang(王小宇)[1], Zhongmin Huang(黄钟民)[1], Haibin Zhao(赵海斌)[1,2], and Jun Wang(王俊)[1,2,†]

[1] *Key Laboratory of Micro & Nano Photonic Structures, Department of Optical Science and Engineering, School of Information Science and Technology, Fudan University, Shanghai* 200433, *China*

[2] *State Key Laboratory of Photovoltaic Science and Technology, Shanghai Key Laboratory of Metasurfaces for Light Manipulation, Shanghai Engineering Research Centre of Ultra Precision Optical Manufacturing, Fudan University, Shanghai* 200433, *China*

(Received 7 April 2025; revised manuscript received 26 May 2025; accepted manuscript online 27 May 2025)

Microcavity exciton-polaritons, formed by strong light–matter coupling, are essential for realizing Bose–Einstein condensation and low-threshold lasing. Such polaritonic lasing and condensation have been demonstrated in III–V semiconductors at liquid helium temperatures. However, the complex fabrication of these microcavities and operating temperatures limit their room-temperature practical application. Here, we experimentally realize room-temperature exciton-polariton condensation and polaritonic lasing in a $CsPbBr_3$ perovskite planar microcavity fabricated by the pressing process. Angle-resolved photoluminescence spectra demonstrate the strong light–matter coupling and the formation of exciton-polaritons in such a pressed microcavity. Above the critical threshold, mass polaritons accumulating at the bottom of dispersion lead to a narrow emission linewidth and pronounced blueshift, further reinforcing the Bose–Einstein condensation and polaritonic lasing in this system. Our results offer a feasible and effective approach to investigate exciton-polariton condensation and polariton lasing at room temperature.

Keywords: exciton-polariton, polariton condensation, perovskite semiconductors, optical microcavity

PACS: 42.50.Pq, 71.36.+c, 42.55.Sa

DOI: 10.1088/1674-1056/addce6 **CSTR:** 32038.14.CPB.addce6

1. Introduction

Microcavity exciton-polaritons, the quasiparticles arising from the strong coupling between excitons and photons, possess unique properties due to their hybrid nature, including low effective mass, strong nonlinearity, long-range coherence, and so on.[1] These characteristics result in the realization of various macroscopic quantum phenomena, such as quantum fluids,[2] quantum vortex,[3,4] spin–orbit effects,[5] solitons,[6] and Bose–Einstein condensation (BEC).[7–9] Among these phenomena, polariton condensation has attract significant attraction, as it provides a platform for studying quantum coherence and enables low-threshold lasing without population inversion,[1] in contrast to traditional photonic lasing. Polariton lasing has initially been realized in III–V semiconductor microcavities such as GaAs[10] and CdTe[7] at cryo-temperature owing to their small exciton binding energy. However, the low operating temperatures have significantly limited the practical applications of polaritonic devices.

Recently, the operating temperature of polariton lasing has been raised to room temperature by utilizing gain materials such as ZnO,[11] GaN,[12] transition metal dichalcogenides (TMDs),[13] and perovskite semiconductors.[14] These kinds of emerging materials with larger exciton bonding energy and larger oscillator strength enable the enhancement of polariton coupling at higher temperatures. However, the fabrication of ZnO and GaN usually needs complex procedures,[11,12] hindering the fabrication of plate microcavities. While TMDs exhibit great nonlinear interaction strength and exciton stability,[13] the lasing and condensation of their monolayers are challenged,[15] limiting the exciton-polariton study within the nonlinear regime. Perovskite semiconductors rely on easy fabrication[16] and excellent optical characteristics, such as high optical absorption,[17] a broad tunable range of emission wavelength,[18] and large exciton binding energy, making them extensively used in light-emitting diodes[19,20] and integrated photonics devices,[21] which are a suitable platform to investigate strong light–matter coupling and exciton-polaritons.

Optical microcavities can confine resonant photons, offering a resonator to enhance the interaction between exciton and photon in the exciton-polariton systems. In recent years, via multiple synthesis methods of microstructures, perovskite semiconductors have been incorporated into various microcavities, including Fabry–Pérot (FP) cavities,[22–24] whispering gallery mode (WGM) resonators,[25] and photonic crystals[26,27] to realize the polariton laser.

†Corresponding author. E-mail: wangjunfd@fudan.edu.cn

© 2025 Chinese Physical Society and IOP Publishing Ltd. All rights, including for text and data mining, AI training, and similar technologies, are reserved.

However, photonic crystals and WGM resonators require lithography and etching processes, which will damage the gain material or reduce its photoluminescence (PL) quantum yield. Conversely, FP cavities offer a simpler and more practical approach, enabling strong exciton–photon coupling with minimal damage and reduced optical losses. Traditional FP cavities are made by depositing highly reflective layers, including distributed Bragg reflectors (DBRs) and metal mirrors.[28,29] This process requires high temperatures, which will destroy the gain materials. Open cavities provide a promising alternative[30] to precise control of cavity length and detuning. However, their fabrication also faces challenges, primarily due to the requirement for ultra-precise positioning mechanisms and fine-step actuators, for example piezoelectric ceramics, making the process technically demanding and costly.

In this work, we fabricate perovskite FP planar microcavity by a harmless pressing method and employing $CsPbBr_3$ perovskite thin film as the gain material. Within the pressed planar microcavity, we demonstrate exciton-polariton condensation and polariton lasing at room temperature. Below the lasing threshold, the analysis of angle-resolved spectra reveals the exciton-polariton exhibits anti-cross behaviors. Above the threshold, power-dependent emission further demonstrates the nonlinear behavior of exciton-polariton condensation and lasing, including enhanced intensity, narrowed linewidth, and notable blueshift. Our results prove the feasibility of room-temperature polariton lasing in harmlessly pressed FP cavities and pave a promising way for developing room-temperature polaritonic lasers.

2. Fabrication and optical characterization of perovskite pressed microcavity

The microcavity structure is schematically shown in Fig. 1(a), consisting of a $CsPbBr_3$ thin film and a pair of highly reflective DBRs. The bottom DBR (10.5 pairs of SiO_2/TiO_2 layers) and the top DBR (8.5 pairs of SiO_2/TiO_2 layers) were deposited on a quartz substrate by an electron beam evaporator. The $CsPbBr_3$ thin film is synthesized by the chemical vapor deposition method and then transferred to the bottom DBR layer by a wet transfer process.[31] To enhance coupling efficiency and prevent environmental degradation, the perovskite layer is spin-coated with a thin photoresist layer. The top and bottom DBRs are bonded with an ultraviolet adhesive to form the FP perovskite microcavity, while the adhesive was dipped to the edge of the DBRs and solidified under the UV light ($\lambda = 365$ nm).

To investigate fluorescence emissions of the perovskite thin film and FP cavity, we nonresonantly pumped the samples using a 457 nm continuous wave laser and measured the PL spectrum at room temperature and low pump fluence. The emission was collected into a spectrometer and dispersed through a 600 lines/mm grating for spectral analysis. The PL spectra of $CsPbBr_3$ thin film without and within the FP cavity are shown in Fig. 1(b). The PL of $CsPbBr_3$ thin film transferred on a silica substrate (blue curve) shows an emission centered at approximately 2.37 eV (523 nm) with the linewidth of 82 meV. The yellow curve represents the PL emission modulated by the FP cavity and exhibits a sharp peak at 2.23 eV with a pronounced narrow linewidth of 2.34 meV. The extracted $\lambda/\Delta\lambda \sim 1000$ indicates strong optical confinement and PL enhancement, contributing to the coupling between excitons and cavity photons.

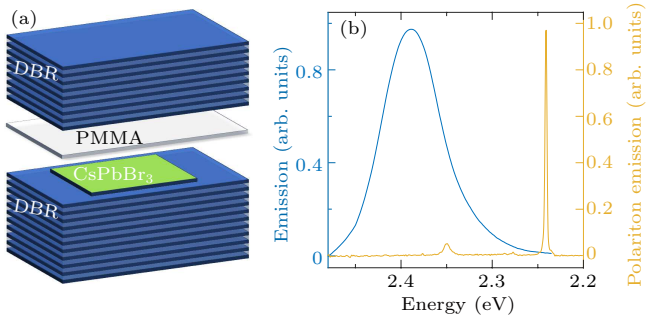


Fig. 1. Microcavity structure and PL emission. (a) Schematic of the perovskite planar microcavity. (b) Room-temperature PL spectra of the perovskite thin film (blue curve) and the perovskite microcavity (yellow curve).

3. Strong light–matter coupling and exciton-polariton dispersion

To prove the existence of strong light–matter coupling and exciton-polaritons in the pressed FP cavity, the polariton dispersion was studied by angle-resolved PL (ARPL) spectra and the coupled oscillator model. The Hamiltonian of the strong light–matter coupling system[32] can be described as

$$H = \begin{pmatrix} E_{\mathrm{ex}} & g \\ g & E_{\mathrm{cavity}} \end{pmatrix}, \tag{1}$$

where E_{ex} is the energy of exciton, E_{cavity} is the resonant energy of the pure cavity photon, and g denotes the coupling strength between exciton and photon, commonly referred to as Rabi splitting energy. The energy of in-plane free exciton and photon could be expressed as $E_i = \hbar^2 k_{\parallel}^2 / 2m_i^*$. Here $\hbar$ is the reduced Planck constant, $k_{\parallel}$ is the in-plane wavevector, and m_i^* means the effective mass, where i refers to the exciton or photon. Due to the larger effective mass than that of photons, excitons exhibit a nearly flat dispersion, while the photon dispersion follows a parabolic dispersion. The solved eigenvalues of such Hamiltonian can be used to describe the dispersion of the upper E_+ and lower polariton branches (LPB) E_- as

$$\begin{aligned} 2E_{\pm}\left(k_{\parallel}\right) = \frac{1}{2}\Big[& E_{\mathrm{ex}}\left(k_{\parallel}\right) + E_{\mathrm{c}}\left(k_{\parallel}\right) \\ & \pm \sqrt{4g^2 + \left(E_{\mathrm{ex}}\left(k_{\parallel}\right) - E_{\mathrm{c}}\left(k_{\parallel}\right)\right)^2}\Big]. \end{aligned} \tag{2}$$

In experiments, we further studied the dispersion properties by ARPL, measured with a home-built micro-PL Fourier

optics imaging setup and collected by a 50× objective lens (numerical aperture, NA = 0.75). Figures 2(a) and 2(b) depict the ARPL spectra of TM mode and TE/TM contrast distribution, respectively. The TE/TM contrast distribution is the estimated S_1 parameter, calculated by $(I_{TE} - I_{TM})/(I_{TE} + I_{TM})$, where I denotes the PL intensity of TE or TM. The dispersions of TE and TM modes showcase an energy difference arising from the intrinsic anisotropy of the $CsPbBr_3$thin film. A notable anti-crossing behavior can be observed at $k_{\parallel} = \pm 6\ \mu m^{-1}$ in the dispersion of Fig. 2(a), as a result of the strong coupling between exciton and photon. The fitted LPB dispersion is depicted as the white dashed line in Fig. 2(a) which aligns with the experiment. The calculated cavity photon mode E_c, with a ground state energy ($k_{\parallel} = 0$) of 2.307 eV, is presented by a dashed line, while the straight line labeled E_x represents the exciton energy of 2.41 eV. In this case, with a negative detuning of $\Delta = E_c - E_{ex} = -101$ meV, the fitted Rabi splitting energy is 117 meV, which is a larger value in the room-temperature polariton system.

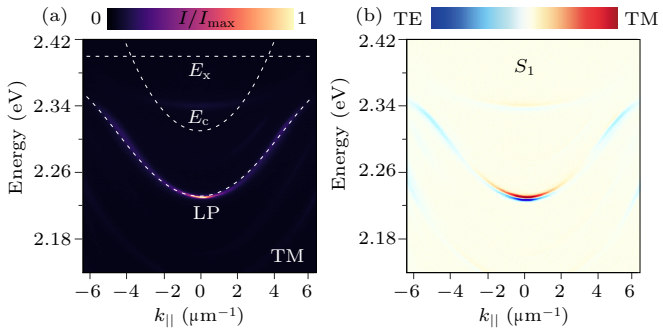


Fig. 2. ARPL of $CsPbBr_3$ perovskite microcavity at room temperature. (a) TM-polarization mode, the dashed curves showing the fitted dispersion of exciton, cavity, and LPB. (b) Dispersion of Stokes parameter S_1.

4. Room-temperature exciton-polariton condensation and lasing

To further study room-temperature condensation and polaritonic lasing in the strong exciton–light coupling regime, the pressed microcavity was non-resonantly pumped by a femtosecond pulsed laser at 400 nm with a repetition rate of 1 kHz and a pump spot with a diameter of 12 μm. Due to insufficient peak power and thermal effects, continuous wave laser excitation could not supply a sufficient polariton density to form condensation. Figure 3 shows the ARPL of polariton emission at pump fluences of $0.72P_{th}$, $1.0P_{th}$, and $1.2P_{th}$ (the threshold $P_{th} = 194\ \mu J \cdot cm^{-2}$) of TM modes, respectively. Under low pump fluence of $0.72P_{th}$, the dispersion flattens in higher momentum k (Fig. 3(a)), owing to the anti-crossing behavior and the exciton-component increasing. All states of LPB are occupied. With the pump fluence increasing over the threshold (Figs. 3(b) and 3(c)), stimulated scattering dominates the polariton dynamics, leading to macroscopic occupation at the ground state of LPB with a narrow momentum distribution, signaling the onset and establishment of polariton condensation. At the pump fluence of $1.2P_{th}$, the emission peak of condensates at $k_{\parallel} = 0$ slightly shifts to higher energy, i.e., a blueshift of 1.2 meV, arising from the nonlinear repulsive interactions of both polariton–polariton and polariton–exciton reservoir, which drive the polaritons to higher energies. Such a blueshift serves as a key signature of the polariton condensation. The emergence of blueshift and concentrated momentum distribution serve as clear evidences of polariton condensation.

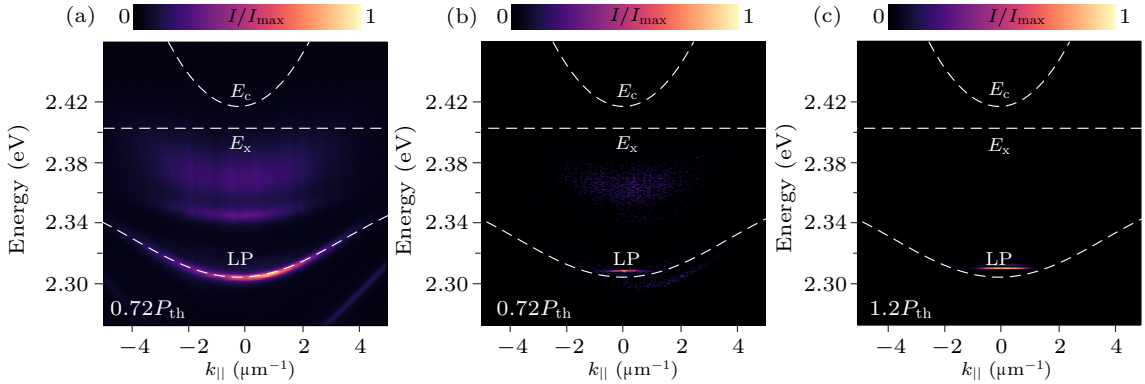


Fig. 3. Power-dependent ARPL spectra: (a) below the threshold at $0.72P_{th}$, (b) at $1.0P_{th}$, (c) above the threshold at $1.2P_{th}$, displaying mass population occupation at $k_{\parallel} = 0$ and an energy blueshift of 1.2 meV.

As condensation occurs, the systems exhibit nonlinear characteristics and the transition from spontaneous emission to stimulated polariton lasing. To confirm this phenomenon, the evolution of the PL intensity, linewidth, and energy blueshift as a function of pumping fluence was investigated by extracting the emission parameter from the ground state. When the pump fluence exceeds the threshold P_{th}, the PL intensity superlinearly increases by two orders of magnitude, as shown in Fig. 4(a). Simultaneously, due to the stimulated scattering and bosonic condensation, the linewidth significantly narrows from 13 meV to 0.5 meV, in which the spectral narrowing has a $\lambda/\Delta\lambda$ factor estimated to be 4600. These two features indicate the high monochromaticity and the appearance of lasing behavior. Furthermore, different from conventional photonic lasing, the polariton lasing exhibits pronounced energy blueshift above the threshold, with a shift of 5 meV com-

pared to the below-threshold states (Fig. 4(b)). If the pump fluence was increased to extremely high level, the emission intensity would gradually saturate. In such a situation, exciton-polaritons would begin to decouple due to exciton dissociation to unbound electron–hole plasma,[33] reducing the efficiency of the strong light–matter coupling. This decoupling process would weaken the condensate coherence and ultimately impact the stability of polariton lasing at extremely high excitation densities.

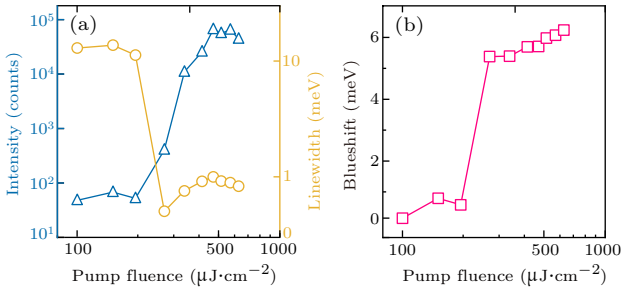


Fig. 4. Lasing characterizations of perovskite microcavity polariton. (a) Integrated emission intensity (blue) and linewidth (yellow) as a function of the pump fluence, showing the threshold of $P_{\text{th}} = 194\ \mu\text{J}\cdot\text{cm}^{-2}$. (b) The blueshift of polariton emission as a function of the pump fluence.

5. Conclusion

In conclusion, we have successfully fabricated a high-quality FP microcavity by using a UV adhesive pressed method, which preserves the integrity of the gain material. By utilizing an all-inorganic $CsPbBr_3$ perovskite thin film as a gain and employing its high exciton binding energy and strong PL advantage, we achieved strong exciton–photon coupling, polariton condensation, and polariton lasing at room temperature. The observed lasing is characterized by a macroscopic occupation of the ground state, an enhanced emission intensity, a pronounced energy blueshift, and a $\lambda/\Delta\lambda$ of 4600. Compared to conventional fabrication methods, our approach offers a simpler, low-cost, and highly efficient method to construct the active FP microcavities and realize room-temperature exciton polariton and their condensation. Our results provide a promising pathway toward the development of polariton lasing devices and integrated on-chip coherent light sources at room temperature.

Acknowledgements

The authors gratefully acknowledge the support from the National Natural Science Foundation (Grant No. 12204111), the National Key Research and Development Program of China (Grant No. 2023YFA1407100), and Shanghai Pilot Program for Basic Research (Grant No. 22JC1403202).

References

[1] Kavokin A 2010 *Phys. Status Solidi B Basic Res.* **247** 1898
[2] Sanvitto D, Pigeon S, Amo A, Ballarini D, De Giorgi M, Carusotto I, Hivet R, Pisanello F, Sala V G, Guimaraes P S S, Houdré R, Giacobino E, Ciuti C, Bramati A and Gigli G 2011 *Nat. Photonics* **5** 610
[3] Dominici L, Carretero-González R, Gianfrate A, Cuevas-Maraver J, Rodrigues A S, Frantzeskakis D J, Lerario G, Ballarini D, De Giorgi M, Gigli G, Kevrekidis P G and Sanvitto D 2018 *Nat. Commun.* **9** 1467
[4] Wang J, Peng Y, Xu H, Feng J, Huang Y, Wu J, Liew T C H and Xiong Q 2022 *Natl. Sci. Rev.* **10** nwac096
[5] Li Y, Ma X, Zhai X, Gao M, Dai H, Schumacher S and Gao T 2022 *Nat. Commun.* **13** 3785
[6] Septembre I, Foudjo I, Develay V, Guillet T, Bouchoule S, Zúñiga-Pérez J, Solnyshkov D D and Malpuech G 2024 *Phys. Rev. B* **109** 205302
[7] Kasprzak J, Richard M, Kundermann S, Baas A, Jeambrun P, Keeling J M J, Marchetti F M, Szymańska M H, André R, Staehli J L, Savona V, Littlewood P B, Deveaud B and Dang L S 2006 *Nature* **443** 409
[8] Deng H, Haug H and Yamamoto Y 2010 *Rev. Mod. Phys.* **82** 1489
[9] Su R, Fieramosca A, Zhang Q, Nguyen H S, Deleporte E, Chen Z, Sanvitto D, Liew T C H and Xiong Q 2021 *Nat. Mater.* **20** 1315
[10] Bajoni D, Senellart P, Wertz E, Sagnes I, Miard A, Lemaître A and Bloch J 2008 *Phys. Rev. Lett.* **100** 047401
[11] Li F, Orosz L, Kamoun O, Bouchoule S, Brimont C, Disseix P, Guillet T, Lafosse X, Leroux M, Leymarie J, Mexis M, Mihailovic M, Patriarche G, Réveret F, Solnyshkov D, Zuniga-Perez J and Malpuech G 2013 *Phys. Rev. Lett.* **110** 196406
[12] Guillet T and Brimont C 2016 *C. R. Phys.* **17** 946
[13] Zhao J, Su R, Fieramosca A, Zhao W, Du W, Liu X, Diederichs C, Sanvitto D, Liew T C H and Xiong Q 2021 *Nano Lett.* **21** 3331
[14] Su R, Wang J, Zhao J, Xing J, Zhao W, Diederichs C, Liew T C H and Xiong Q 2018 *Sci. Adv.* **4** eaau0244
[15] Zhao B, Shen D, Zhang Z, Lu P, Hossain M, Li J, Li B and Duan X 2021 *Adv. Funct. Mater.* **31** 2105132
[16] Elangovan N K, Kannadasan R, Beenarani B B, Alsharif M H, Kim M -K and Hasan Inamul Z 2024 *Energy Rep.* **11** 1171
[17] Monama G R, Ramohlola K E, Iwuoha E I and Modibane K D 2022 *Results Chem.* **4** 100321
[18] Protesescu L, Yakunin S, Bodnarchuk M I, Krieg F, Caputo R, Hendon C H, Yang R X, Walsh A and Kovalenko M V 2015 *Nano Lett.* **15** 3692
[19] Li J, Du P, Guo Q, Sun L, Shen Z, Zhu J, Dong C, Wang L, Zhang X, Li L, Yang C, Pan J, Liu Z, Xia B, Xiao Z, Du J, Song B, Luo J and Tang J 2023 *Nat. Photonics* **17** 435
[20] Lin K, Xing J, Quan L N, de Arquer F P G, Gong X, Lu J, Xie L, Zhao W, Zhang D, Yan C, Li W, Liu X, Lu Y, Kirman J, Sargent E H, Xiong Q and Wei Z 2018 *Nature* **562** 245
[21] Han Q, Wang J, Tian S, Hu S, Wu X, Bai R, Zhao H, Zhang D W, Sun Q and Ji L 2024 *Nat. Commun.* **15** 1536
[22] Song J, Ghosh S, Deng X, Li C, Shang Q, Liu X, Wang Y, Gao X, Yang W, Wang X, Zhao Q, Shi K, Gao P, Xing G, Xiong Q and Zhang Q 2025 *Sci. Adv.* **11** eadr1652
[23] Zou C, Cao X, Wang Z, Yang Y, Lian Y, Zhao B and Di D 2025 *Sci. Adv.* **11** eadr8826
[24] Su R, Diederichs C, Wang J, Liew T C H, Zhao J, Liu S, Xu W, Chen Z and Xiong Q 2017 *Nano Lett.* **17** 3982
[25] Zhang Q, Su R, Liu X, Xing J, Sum T C and Xiong Q 2016 *Adv. Funct. Mater.* **26** 6238
[26] Wang D, Albert Y X, Zhang J Q, She Z D, Kang X F, Zhu Y, Sanjib G and Xiong Q 2024 *Chin. Phys. B* **33** 128103
[27] Ardizzone V, Riminucci F, Zanotti S, Gianfrate A, Efthymiou-Tsironi M, Suàrez-Forero D G, Todisco F, De Giorgi M, Trypogeorgos D, Gigli G, Baldwin K, Pfeiffer L, Ballarini D, Nguyen H S, Gerace D and Sanvitto D 2022 *Nature* **605** 447
[28] Wang J, Su R, Xing J, Bao D, Diederichs C, Liu S, Liew T C H, Chen Z and Xiong Q 2018 *ACS Nano* **12** 8382
[29] Wang J, Da P, Zhang Z, Luo S, Liao L, Sun Z, Shen X, Wu S, Zheng G and Chen Z 2018 *Nanoscale* **10** 10371
[30] Vadia S, Scherzer J, Thierschmann H, Schäfermeier C, Dal Savio C, Taniguchi T, Watanabe K, Hunger D, Karraï K and Högele A 2021 *PRX Quantum* **2** 040318
[31] Dong W, Dai Z, Liu L and Zhang Z 2024 *Adv. Mater.* **36** 2303014
[32] Coker K, Zheng C, Arhin J R, Agyekum K O B O and Zhang W 2024 *Chin. Phys. B* **33** 037102
[33] Kappei L, Szczytko J, Morier-Genoud F and Deveaud B 2005 *Phys. Rev. Lett.* **94** 147403